Airtightness Enhancement in Flexible OLED Modules Using Mechanically Foamed SCF

Yu Gu*, Sheng Jin**, Renjie Liu*

*** Visionox Technology Inc., KunShan, Jiangsu, China.**
**** Hefei Visionox Technology Co., Ltd., China.**

Abstract

Flexible OLED modules require a buffering backplane to mitigate impact damage. Mechanically frothed foam is a key candidate due to its balanced performance, but its inherent semi-open cell structure poses a challenge for device air/water tightness, risking IP rating failures. This study investigates the root cause of this leakage. We developed a novel testing method and discovered that leakage depends not only on density but crucially on cell size and connectivity. By optimizing the surfactant content to enlarge cell size and reduce density, we achieved a fundamental improvement in air tightness.

Author Keywords

Flexible OLED；SCF；gas-foamed foam；airtightness；pore connectivity； COE；ultrasonic fingerprint.

1. Introduction

In next-generation flexible OLED displays, the backside soft composite film (SCF) plays a critical role in mitigating point pressure and ball-drop impacts, thereby reducing the risk of localized pixel failure such as “bright spots.” However, material selection involves inherent trade-offs between mechanical protection, surface flatness, and environmental sealing.

Traditional acrylic particle foams tend to induce “orange peel” due to discrete closed cells, while emerging adhesive films—such as silicone and acrylic PSAs—often cause “film imprint” under sustained stress. These issues are further intensified in advanced integration schemes: in COE (Color Filter on Encapsulation), the removal of the polarizer (POL) increases stress concentration; in ultrasonic fingerprint modules, film imprint and orange peel are exacerbated after secondary lamination and degassing processes, where thermal cycling amplifies surface non-uniformity.

Mechanically gas-foamed polyolefin foam remains a preferred SCF option due to its excellent balance of conformability, shock absorption, and low imprint. However, its semi-open/closed cell structure and stochastic nucleation during foaming can lead to interconnected pores, forming gas leakage paths. This compromises module-level airtightness, resulting in system-level failure during IP65 or higher waterproof testing.

Empirical attempts—such as increasing cell density (CFD) or foam density—have shown limited success, indicating that average physical properties do not fully predict leakage risk. Instead, pore morphology, including size, distribution, and spatial density, governs interconnectivity probability. This study investigates the root cause through microstructural analysis and establishes a controllable solution via additive modulation.

2. Experimental Analysis

2.1 Airtightness Screening Method: To enable early detection and rapid validation, a water immersion test method was developed to evaluate SCF-level airtightness. Based on system-level failure path analysis (Figure 1), leakage primarily occurs at the camera aperture area covered by SCF, where gas penetrates through interconnected pores in the foam to the FEG or mid-frame interface. To address this, a simulated real-condition test was designed (Figure 2): SCF is laminated onto glass, and the camera area is sealed with adhesive and a pneumatic valve, then immersed in deionized water. A constant pressure (e.g., 45 kPa) is applied; continuous bubbling indicates NG, no bubbles indicates OK. This method replicates key failure paths from full-module testing, enabling fast SCF screening and closed-loop optimization for material and process improvements.

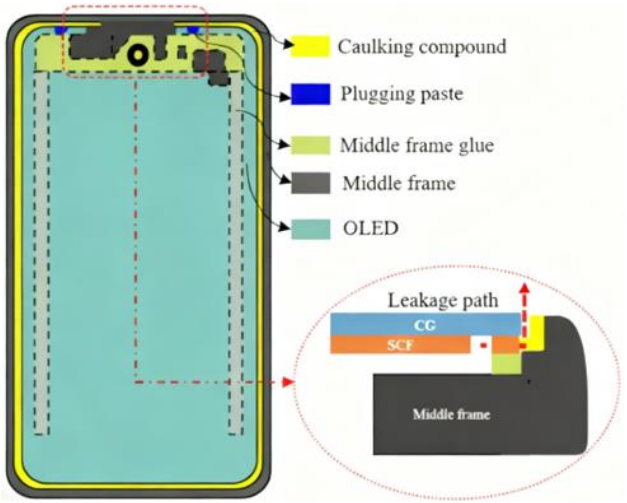

Figure 1. Failure Path Analysis of Module-Level Airtightness Testing

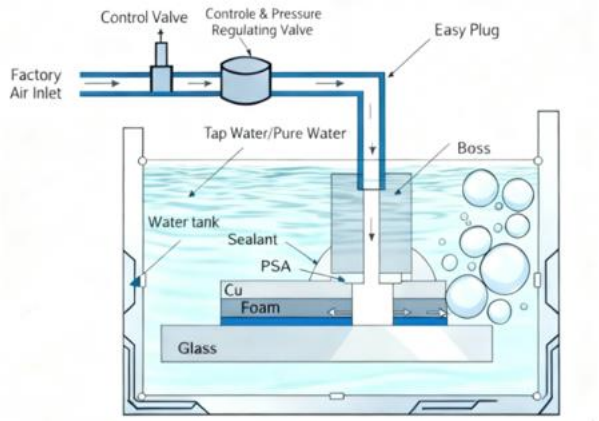

Figure 2. Schematic of SCF-level water immersion test setup

2.2 Effect of CFD and Hardness on Airtightness: First, the influence of overall foam hardness on airtightness was systematically investigated to evaluate whether internal pore structure deformation—induced by test pressure—could alter

pore connectivity and thereby affect sealing performance. To this end, four foam samples with varying CFD (Compression Force Deflection) gradients were fabricated and evaluated under identical testing conditions. As summarized in Table 1, no significant difference in airtightness performance was observed among the four samples. This result indicates that simply increasing CFD or bulk hardness does not effectively enhance airtightness, suggesting that pore-level structural characteristics, rather than macroscopic mechanical properties, play a more critical role in determining sealing integrity.

Table 1. Foam airtightness test results under different CFD conditions

CFD(kpa)	Sample Count	Test air pressure （kpa）	Pass Rate (%)
145	5	20	0
165	5	20	0
190	5	20	0
186	5	20	0

2.3 Effect of Foam Density: Furthermore, an attempt was made to reduce pore connectivity by decreasing the foaming gas volume and increasing the foam density. Two density levels were selected and evaluated under five different blowing pressures. As shown in Table 2, the high-density samples exhibited significantly improved airtightness in small-scale testing, further confirming that airtightness failure is closely associated with interconnected pore structures. However, excessive density may compromise cushioning performance and reduce resistance to film indentation. Therefore, this approach, while effective in mitigating symptoms, does not address the root cause and is thus considered a symptomatic rather than a fundamental solution.

Table 2. Airtightness test performance of foams with different densities

Test air pressure （kpa）	0.73g/cm^3	0.80g/cm^3
20	2/5 NG	0/5 NG
30	5/5 NG	0/5 NG
45	5/5 NG	0/5 NG
100	5/5 NG	0/5 NG

2.4 Microstructural Analysis: Cross-sectional analysis via slicing and SEM imaging revealed distinct morphological differences. NG samples (Figure 3-a) exhibited small, densely packed cells, which increased the probability of interconnected pores between cells as shown in Figure 3-c. In contrast, OK samples (Figure 3-b) showed larger, sparsely distributed cells with greater inter-cell distance, resulting in isolated voids. This indicates that pore size and spatial distribution, rather than bulk density alone, govern gas pathway formation.

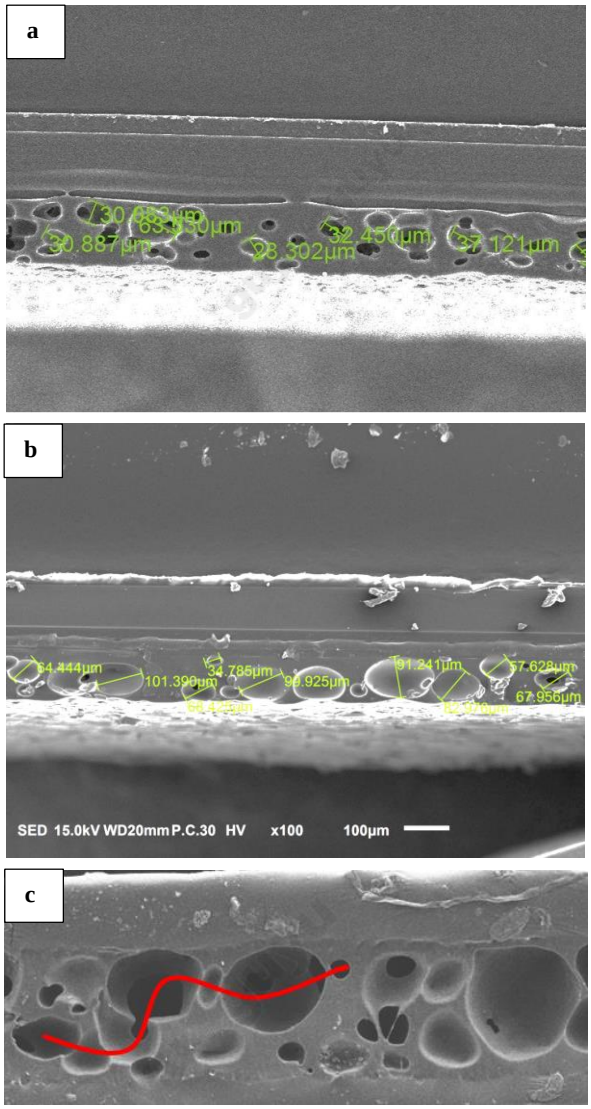

Figure 3. SEM comparison of cross-sectional views of foam cells after slicing for NG and OK samples

2.5 Pore Connectivity Model and Additive Optimization: Based on the findings, a pore connectivity model (Figure 4) was established, with red spheres denoting interconnected (open) cells and blue spheres representing isolated (closed) cells. Airtightness failure results from gas flow (Q) through open pathways driven by pressure differential (Δ P). Under constant foaming gas input (equivalent density), smaller, denser cells increase inter-pore contact probability, enhancing connectivity and degrading airtightness. Thus, precise control of cellular structure is required via material formulation and process optimization.

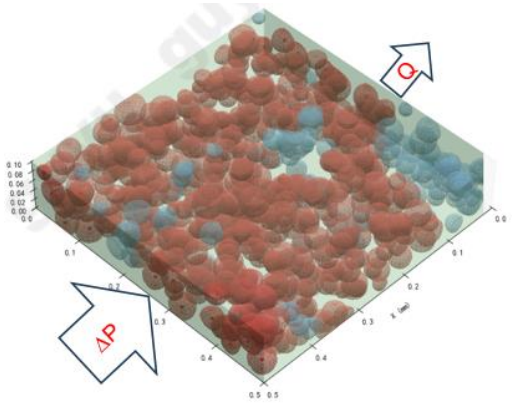

Figure 4. Pore Connectivity Model

To control cell size and distribution, a specific formulation additive was systematically reduced. As shown in Table 3, a clear threshold exists: when additive content was reduced below 46% of the original level, airtightness improved significantly; full pass rate was achieved at 40% and below. This confirms that lower surfactant concentration promotes larger, sparser cells, effectively suppressing pore interconnectivity while maintaining sufficient air content for mechanical performance.

Table 3. Foam airtightness test results under different additive ratios

Additive (% of original)	Test quantity	Pass Rate (%)
100	9	0
86	9	0
73	9	0
60	9	0
53	9	89
46	90	95
40	37	100
33	152	100
26	18	100

As can be observed from Figure 5, there is a significant difference in the cell structure between the foam with 100% additive content and that with 33% additive content. At 33% additive content, the overall cell size increases, the number of cells decreases, and the probability of cell interconnectivity is reduced.

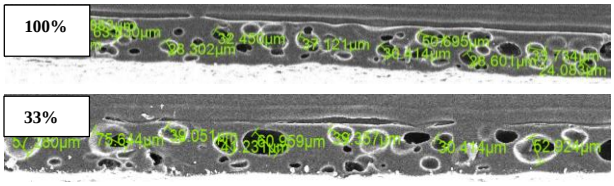

Figure 5. SEM cross-sectional cell comparison of foam at 100% and 33% additive ratios

3. Conclusion and Outlook

By reducing additive ratios, the pore structure of mechanically foamed SCF was optimized to achieve reliable airtightness without sacrificing mechanical performance. This breakthrough enables its use in COE and ultrasonic fingerprint modules, where both defect-free surface quality and IP65+ sealing are required. The solution supports future high-end flexible OLED applications with enhanced environmental robustness and process stability.

4. References

1. Qiao L F, Guo C, Murto P, et al. Design of Monolithic Closed-cell Foams via Controllable Gas-Foaming for High-Performance Solar-Driven Interfacial Evaporation[J]. Journal of Materials Chemistry A, 2021, 9.
2. Zheng W G, Pang Y Y, Park C B. A comprehensive review of cell structure variation and general rules for polymer microcellular foams[J]. Chemical Engineering Journal, 2022, 430: 132662.
3. Wang Jun. Development of a Mobile Phone IP Rating Test Equipment Based on Differential Pressure Leak Detection Principle [D]. Tianjin: Tianjin University, 2014.
4. Zhu Bo. Design and Implementation of a Mobile Phone Waterproof Testing System Based on Direct Pressure Leak Detection Principle [D]. Xi'an: Xidian University, 2019.